Fe-기반 ATF 개발 현황

Alumina-forming duplex stainless (ADSS) 성능평가

장창희, 김채원, 허웅 - KAIST

장훈 - KNF

May 18 (Wed), 2022

Korea Advanced Institute of Science and Technology (KAIST)

Contents

- **Background**
- **Development of alumina-forming duplex SS**
- **Recent assessment of ADSS**
  - Assessment related to accidents
  - Assessment related to normal operation
- **Further assessment in progress**
- **Summary**
- **Extra**

Background

Background

❑ Accident tolerant fuel (ATF) cladding

- Fukushima Daiichi (Japan) nuclear power station accident in March 2011 from tsunami and hydrogen explosion

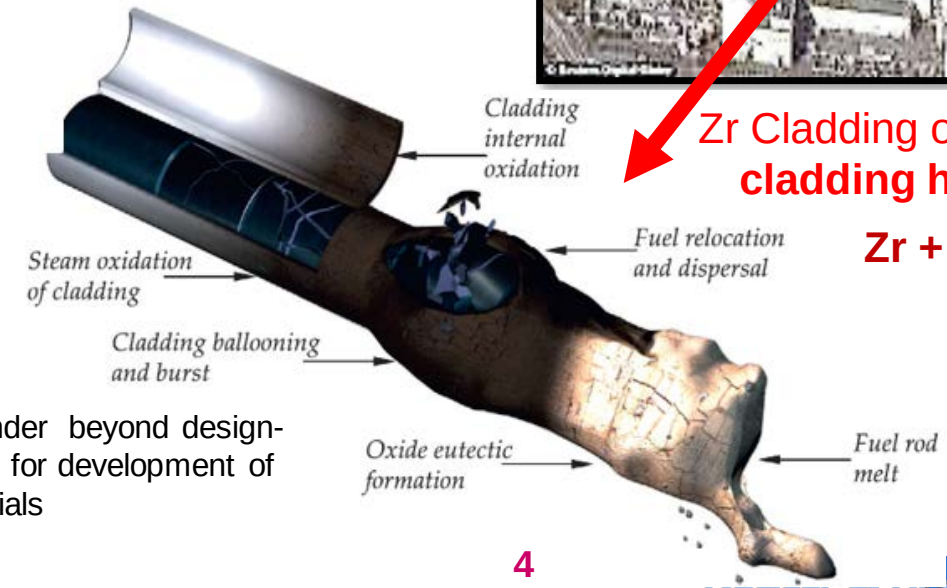

Zr Cladding oxidation: **Major source** of **cladding heating & H generation**

$$Zr + 2H_2O \rightarrow ZrO_2 + 2H_2 + \Delta H$$

▶ Evolution of a fuel rod under beyond design-basis accidents: Motivation for development of ATF materials

Background

S. Maloy et al., Advs. in Nucl. Fuel and Maters. DOE Purdue WS, 2014

❑ Satisfactory steam oxidation resistance

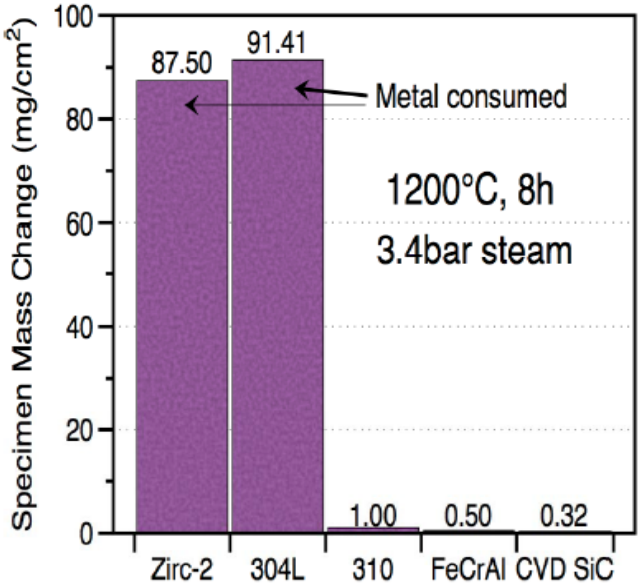

◀ A comparison of conventional alloys and ATF candidate materials in high temp. steam oxidation

BUT!

❑ Some issues of candidate ATF materials

- **Ceramic** cladding (SiC)
  - Brittle fracture in normal operation / Joining
  - Fission products retention issue
- **Coating** on Zr-alloy (Cr/Zr)
  - Inherent Zr behaviors (balloon/burst)
- **Metallic** cladding (Mo, FeCrAl)
  - Poor oxidation (Mo) / Embrittlement (FeCrAl)

⇨ **Better materials for ATF?**

Background - Desired Properties for ATF

Terrani, JNM (2018)

Desired properties

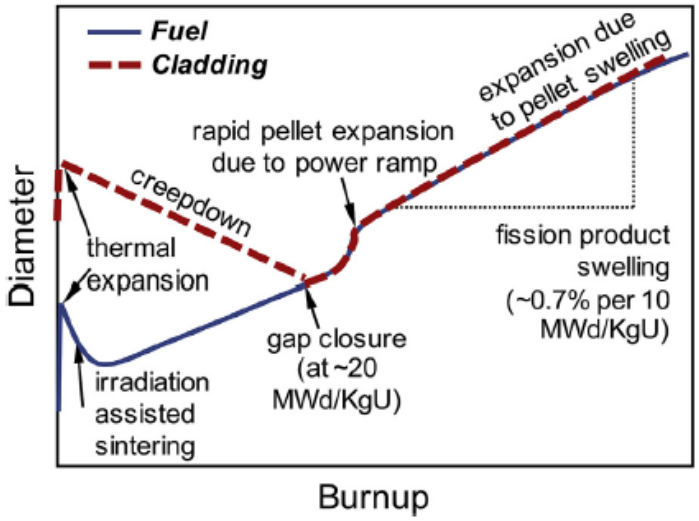

"ADSS"		Cladding				
		NO	PR	LOCA	RIA	SBO
Thermal conductivity	High	↑	↑	↑	-	-
Heat capacity	High	-	-	↑	-	↑
Oxidation rate	Low	↓	↓	↓	↓	↓
Coefficient of thermal expansion		-	-	-	-	-
Creep rate	Low	↑	↑	↓	-	↓
Strength	High	↑	↑	↑	↑	↑
Critical heat flux (CHF)	High	↑	↑	-	↑	-

Benefit of ATF

- Expand fuel operating window (higher CHF, better ductility)
- Increase fuel burnup (not limited by cladding)
- Increase limits on peak cladding temperature under DBA
- Enhanced back-end performance of used fuel

Development of Alumina-forming Duplex SS

Design of ADSS alloys

- Concept of ADSS alloys design
  - High Al for steam oxidation resistance
  - Enough Cr for PWR corrosion resistance
  - Ni addition for better fabrication and embrittlement resistance

Advanced Steel (FeCrAl)

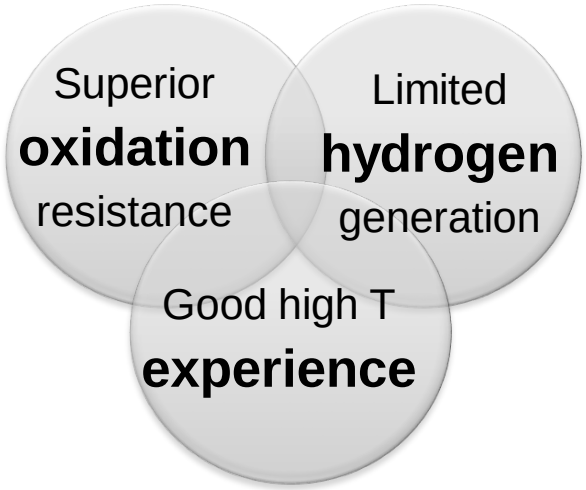

ADSS alloy

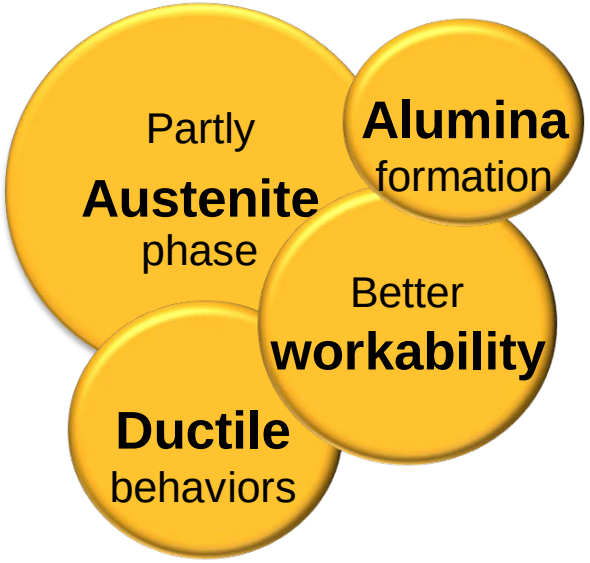

Design of ADSS alloys

H. Kim et al. J. Nucl. Mater., 507 (2018) 1

❑ Composition range

- Fe-(16-20)Ni-16Cr-(5.5-7.0)Al + (Nb, Mn, C, Si)
- Austenite(FCC), ferrite(BCC), nickel aluminide (B2-NiAl) co-exist
- B2-NiAl phase fraction/stability depends on Ni/Al

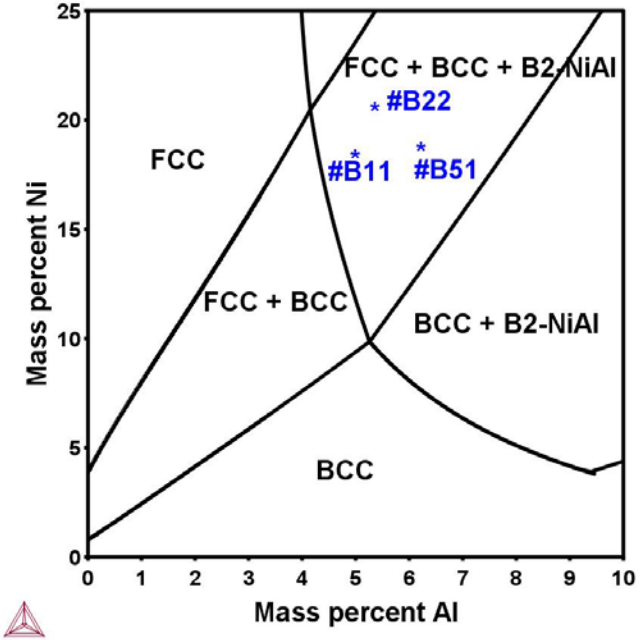

▲ Phase diagram (TCFE-9 database) for Fe-16Cr-xAl-yNi system at 900°C, and the indicated target ADSS compositions

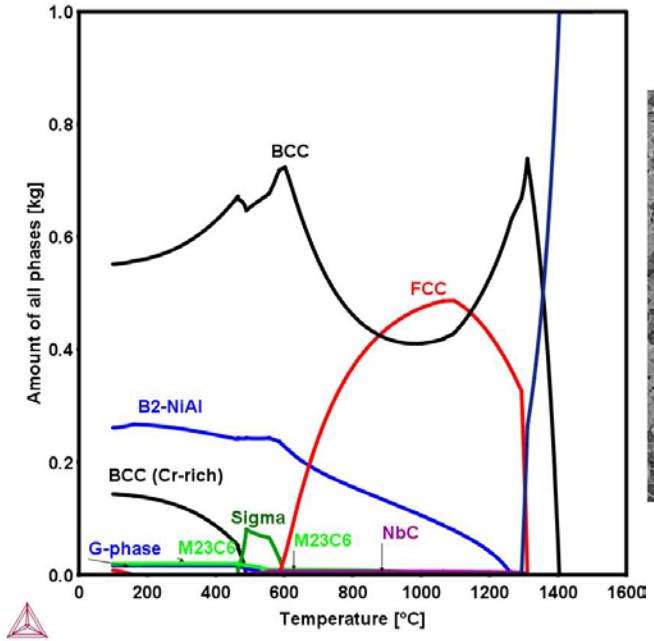

▲ Equilibrium diagram (TCFE-9 database) for predicting the phases of **ADSS #B51 (Fe-19Ni-16Cr-6Al)**

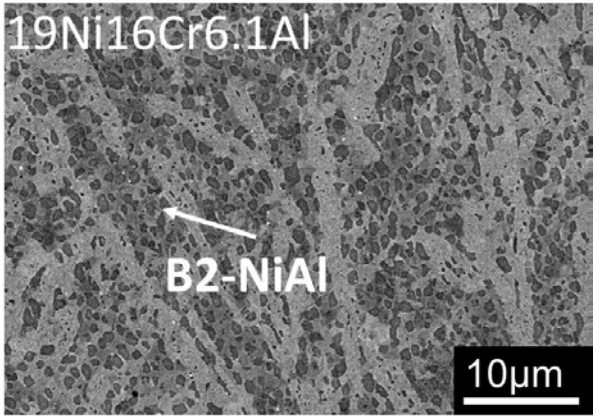

▲ SEM(BSE) image of ADSS #B51 in cold-rolled + final annealed condition

Corrosion/Oxidation of ADSS alloys

❑ High temperature steam oxidation

- Steam TG 1200°C 8h
- ADSS alloys showed somewhat larger weight gain, but with similar kinetics at steady-state
  - Confirmed to form protective alumina formation, comparable to FeCrAl alloys

H. Kim et al. J. Nucl. Mater., 507 (2018) 1

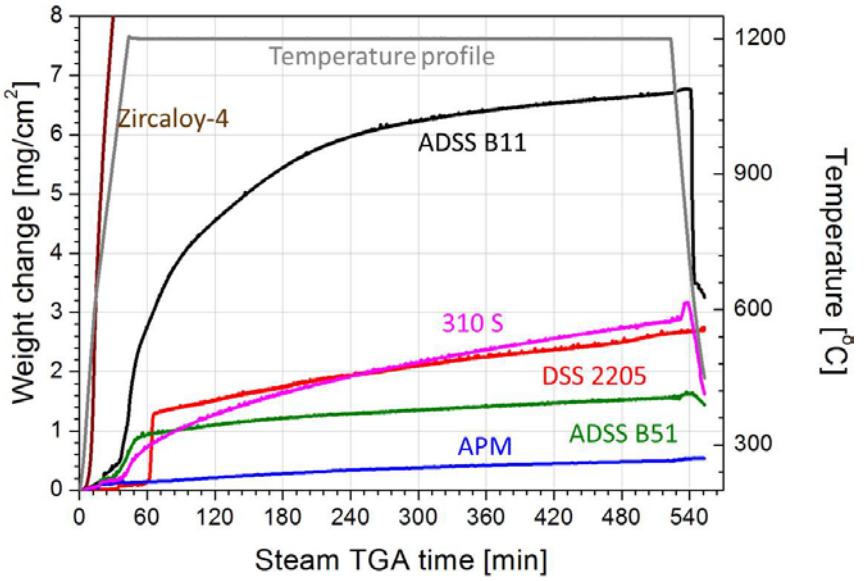

▲ Steam TG graph of ADSS and reference alloys at 1200°C for 8h

❑ PWR corrosion

- Spinel oxides + continuous chromia
- ADSS alloys showed excellent corrosion resistance comparable to 310S SS

Table 6
Mass gain and oxide thickness after 30 days corrosion in the simulated PWR environment.

Materials	Mass gain [mg·dm^{-2}]	Oxide thickness [μm]
ADSS alloys	0.62 ± 0.30	0.05–0.15
APM	−0.33 ± 0.06	–
310 S	Negligible[a]	<0.01
Zircaloy-4	20–30	1.3–2.0[b]

[a] Mass gain less than 0.03 mg dm^{-2}.
[b] Values estimated from the longer-term data.

Tensile properties of ADSS alloys

❑ Mechanical properties

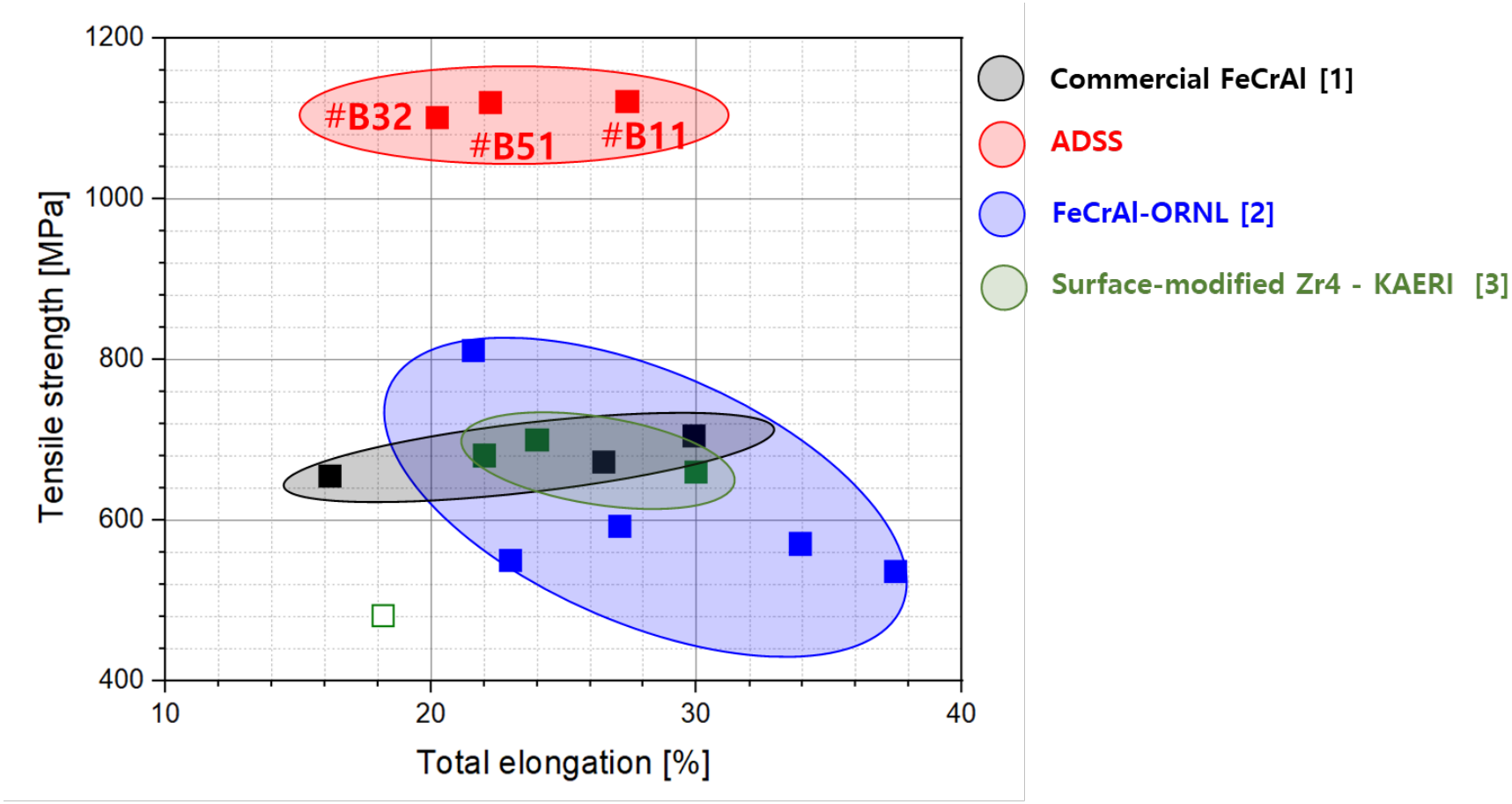

[1] H. Kim et al, Materials Science and Engineering:A 743 (2019) 159-167
[2] Y. Yamamoto et al., Journal of Nuclear Materials 467 (2015) 703-716
[3] H.G. Kim et al, Additive Manufacturing 22 (2018) 75-78

ADSS - Fabrication of thin tubes

❑ Fabrication of thin ADSS tubes

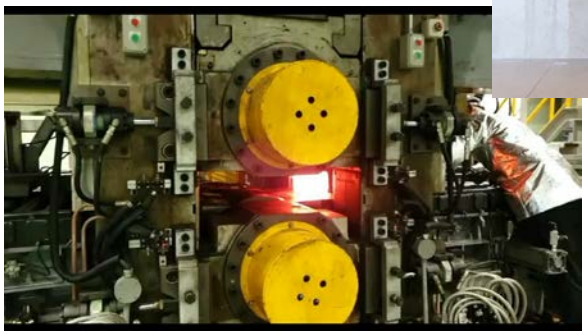

As-cast ingots

Sizing by hot forging and/or rolling

Sized rod

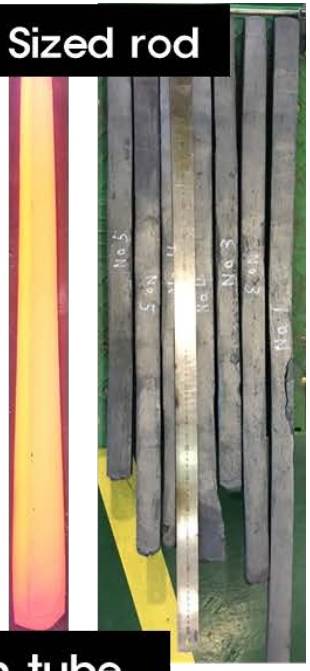

Fabricated bar (master bar)

Thin tube
1.6m O.3t

ADSS - Fabrication of thin tubes

❑ Thin tube fabrication of ADSS

- ~4 m long tube with a thickness of 0.3 mm
  - VIM ingot → hot forging → fabrication of master bar → gun drilling → cold 3-roll pilger
- Uniformly-distributed phases and small grains
- Multi-step pilger process with intermediate and final annealing
  - Trying to reduce steps

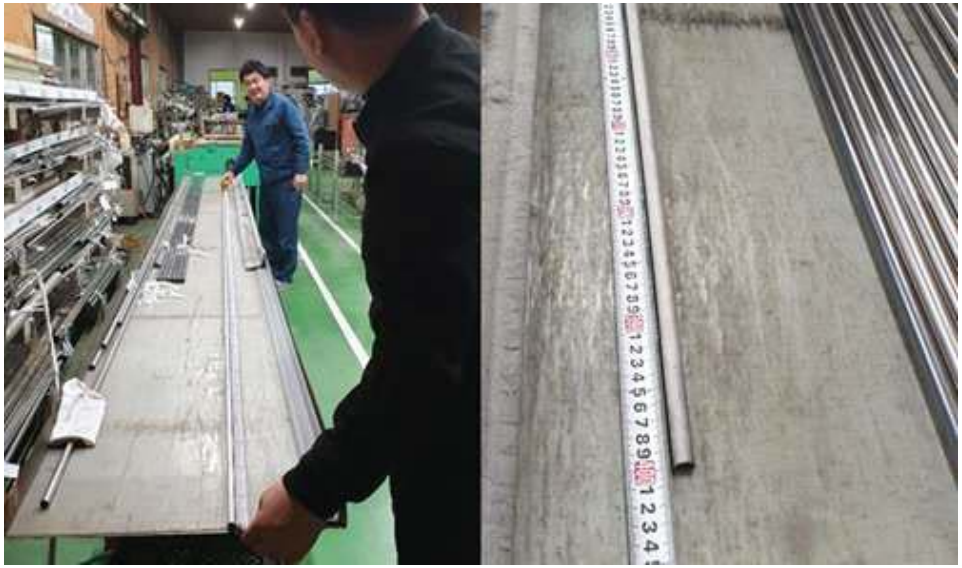

▲ Cold-pilgered ADSS tubes produced by San-ekki worked with KNF

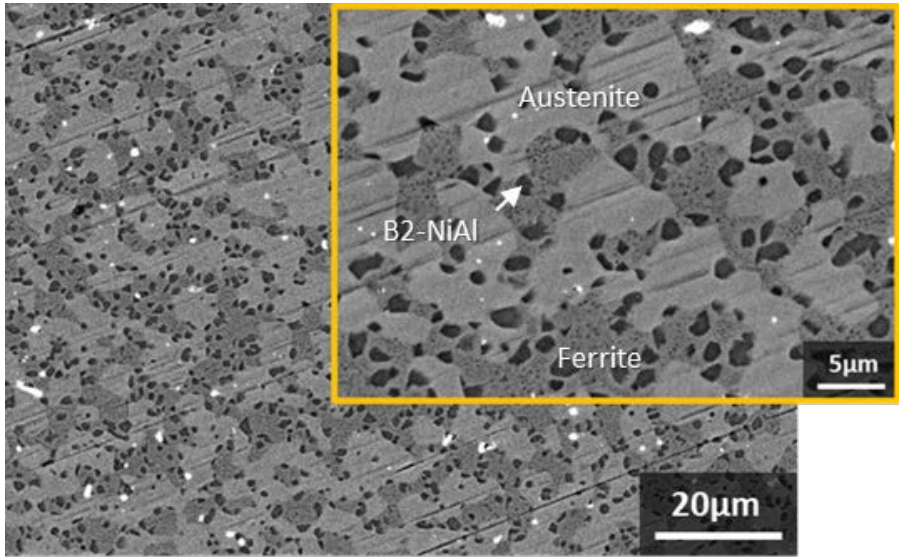

▲ Cross-sectional microstructure of thin ADSS tubes

Recent Assessment of ADSS alloys

Assessment related to accidents

C. Kim et al., Corros. Sci. 190 (2021) 109658

- **Steam oxidation resistance at 800ºC–1050ºC**
  - Similar weight changes with APM at 800-1050ºC
  - T < 1000ºC
    - Mainly Al_2O_3 like FeCrAl
  - 1000ºC < T ≤ 1200ºC
    - Spinel oxides + Al_2O_3
    - But, spinel oxide formation is suppressed after the formation of continuous Al_2O_3

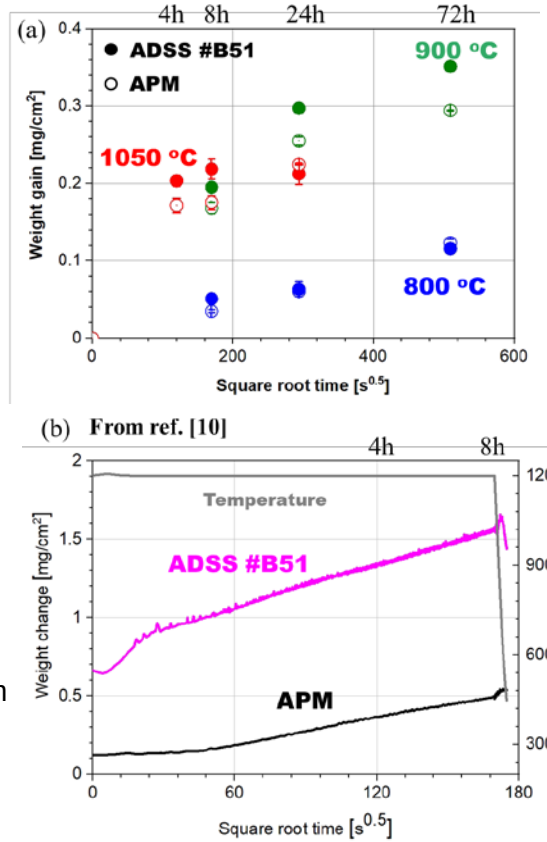

Weight changes as function of square root time ▶ for ADSS #B51 and APM exposed to steam (a) at from 800ºC to 1050ºC and (b) at 1200ºC

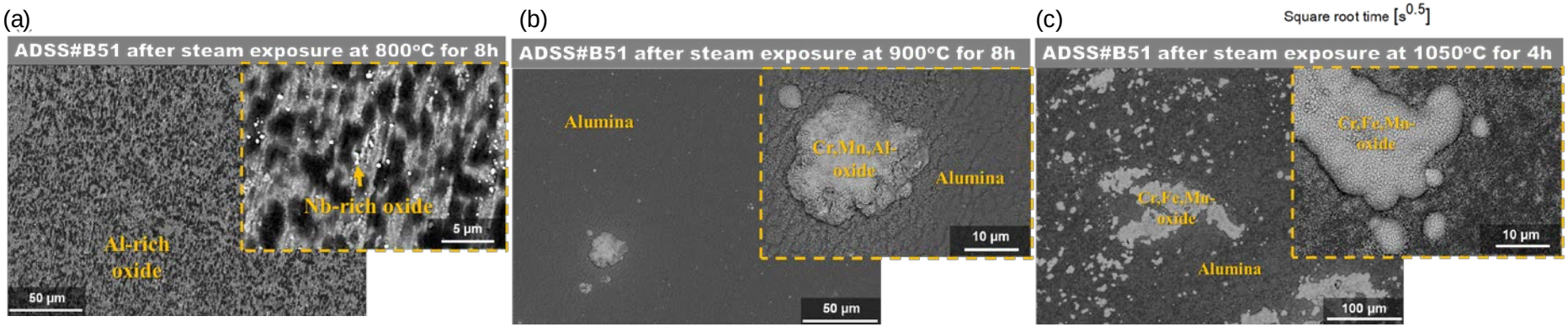

▲ Surface oxide BS-SEM images of ADSS #B51 after steam oxidation test (a) at 800ºC for 8h, (b) at 900ºC for 8h, and (c) at 1050ºC for 4h

Assessment related to accidents

❑ High temperature mechanical properties

- Tensile properties at high temperature
  - Much stronger than FeCrAl alloys
    - UTS ~ 600 MPa up to 500ºC
  - Rapid loss of strength at 600ºC
  - Negligible change in tensile properties at 800ºC after long-term thermal ageing at 400ºC

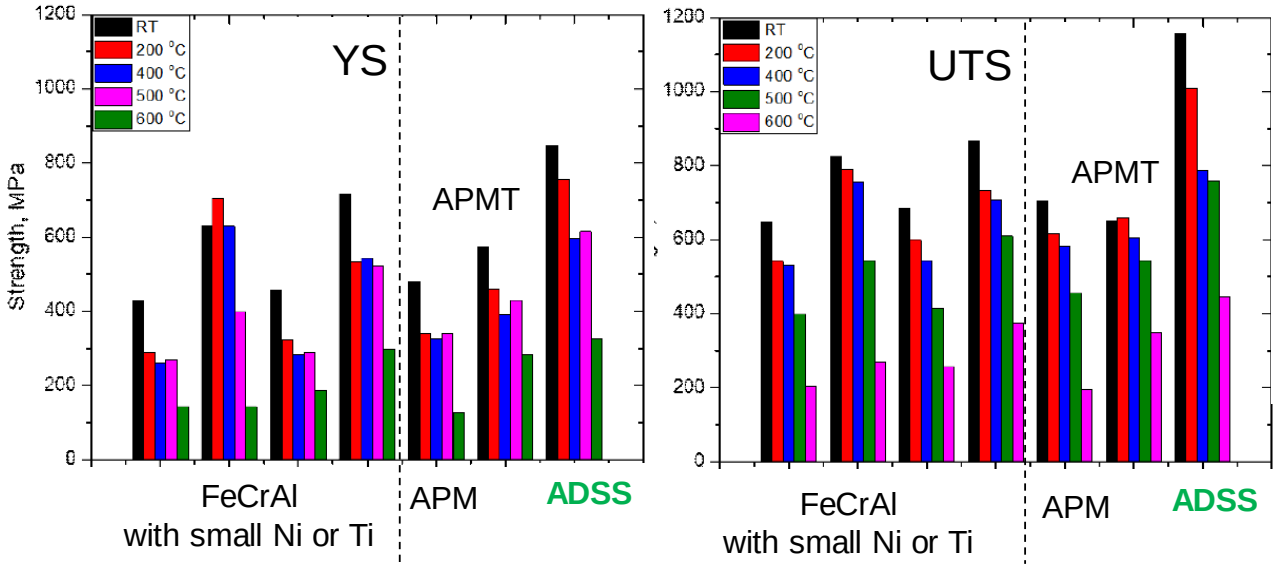

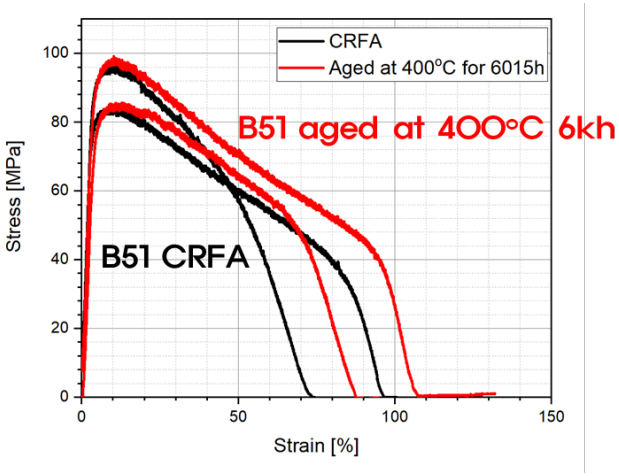

▲ Mini-tensile test results at 800ºC for B51CRFA before and after ageing at 400ºC for 6kh

▲ Tensile properties of FeCrAl alloys and ADSS #B51 at RT to 600ºC: (a) YS and (b) UTS

Assessment related to accidents

❑ High temperature mechanical properties

- Creep test using cladding tubes by KNF
  - 0.35 mm in tube thickness / inert gas and pellet within tubes
  - Tested in vacuum and slightly higher hoop stress than Zr-Nb tubes
- Creep rate comparing with Zr-Nb
  - ~1/16 creep rate of Zr-Nb at 650°C
  - ~1/14 creep rate of Zr-Nb at 1000°C

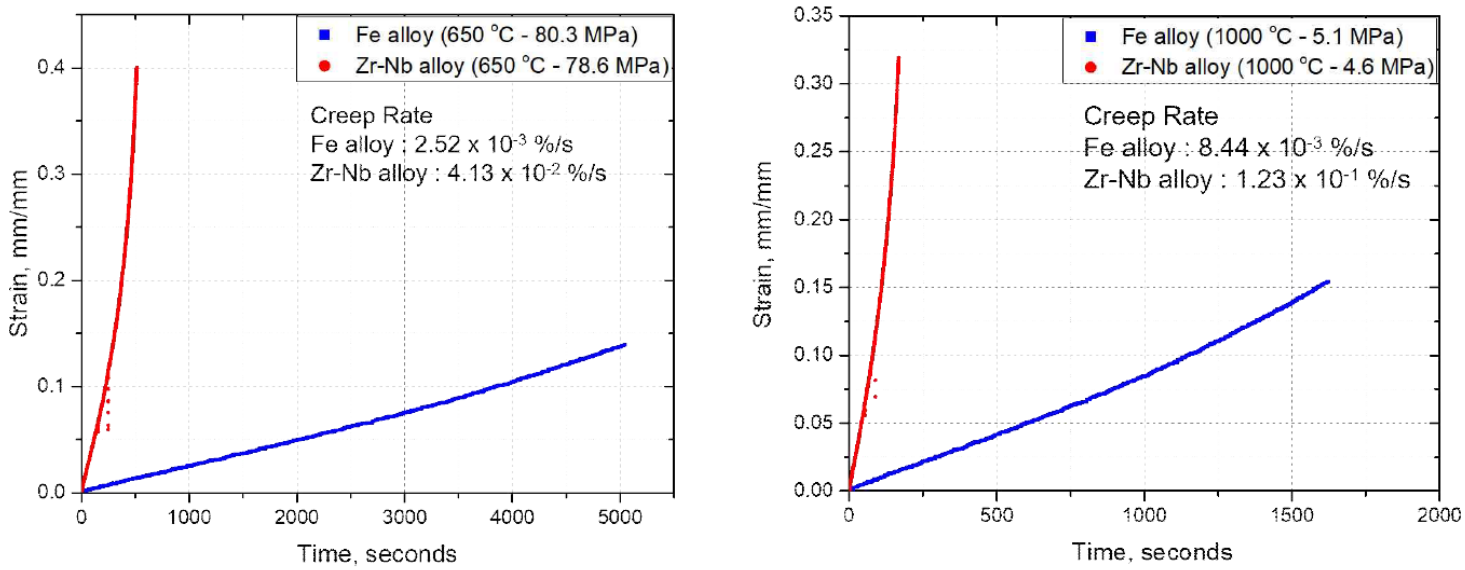

▲ High temperature creep results of ADSS and Zr-Nb alloy (a) at 650°C and (b) at 1000°C

Assessment related to accidents

[1] J. Nucl. Mater. 557 (2021) 153242
[2] J. Nucl. Mater. 564 (2022) 153679

❑ Burst behavior of ADSS

- Burst test condition
  - 0.6 mm in cladding thickness, Ar gas within tube specimens
  - Heating rate of 5°C/min up to 1200°C and hold for 480s
  - When pressure drops, burst T and P are determined
- Burst test result comparing with others
  - When hoop stress ~ 76 MPa, burst temp. for Zr-2 (~700°C) and for FeCrAl (~900°C)
    - ☐ No burst and ballooning yet for ADSS up to 1200°C

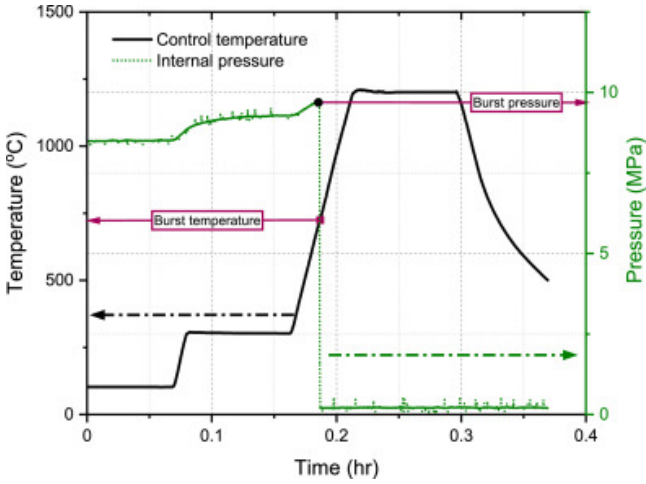

▲ Temperature and pressure profile during burst test

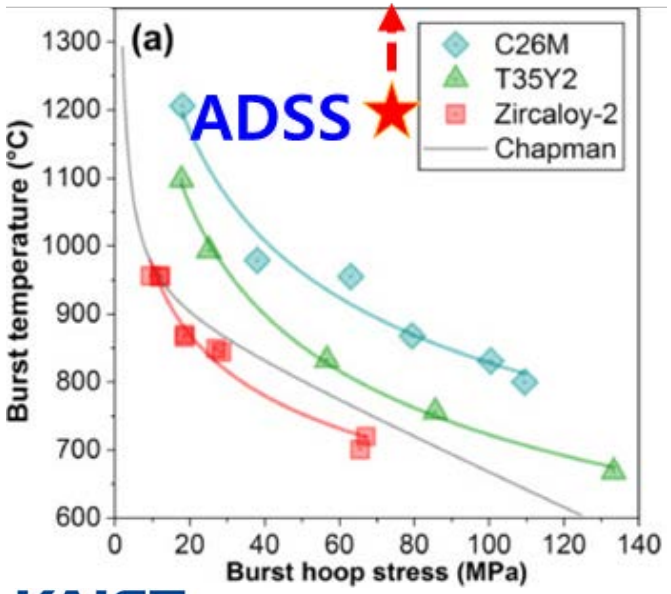

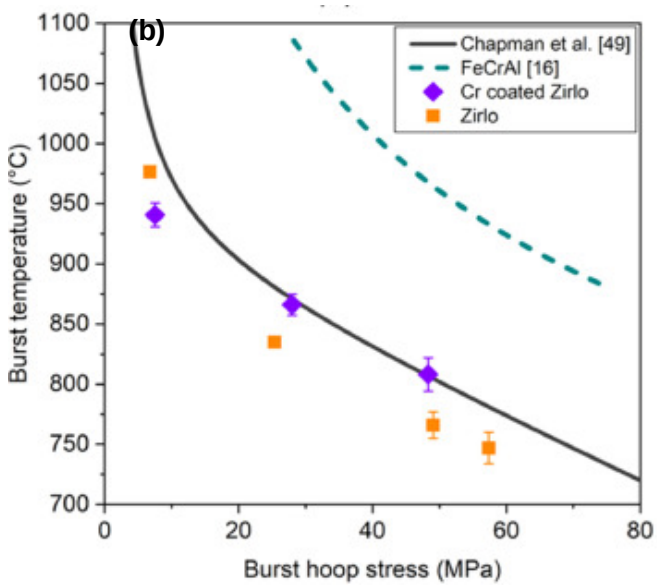

▲ Burst test results of (a) Zr-2 and ORNL-FeCrAl alloys [1] with ADSS burst result and (b) Zirlo and Cr-coated zirlo [2]

Assessment related to normal operation

[1] Q. Xiao et al., Corros. Sci. 177 (2020) 108991

❑ PWR corrosion behavior

- Almost saturated weight changes after 30 days-exposure
- Outer particle : $(Fe, Ni, Al)_3O_4$ spinel
- Inner layer
  - Ferrite : Cr-rich oxide (Cr_2O_3 + $FeCr_2O_4$)
  - Austenite : Cr-rich nano-crystalline spinel
  - Large B2-NiAl: $(Fe, Ni, Al)_3O_4$

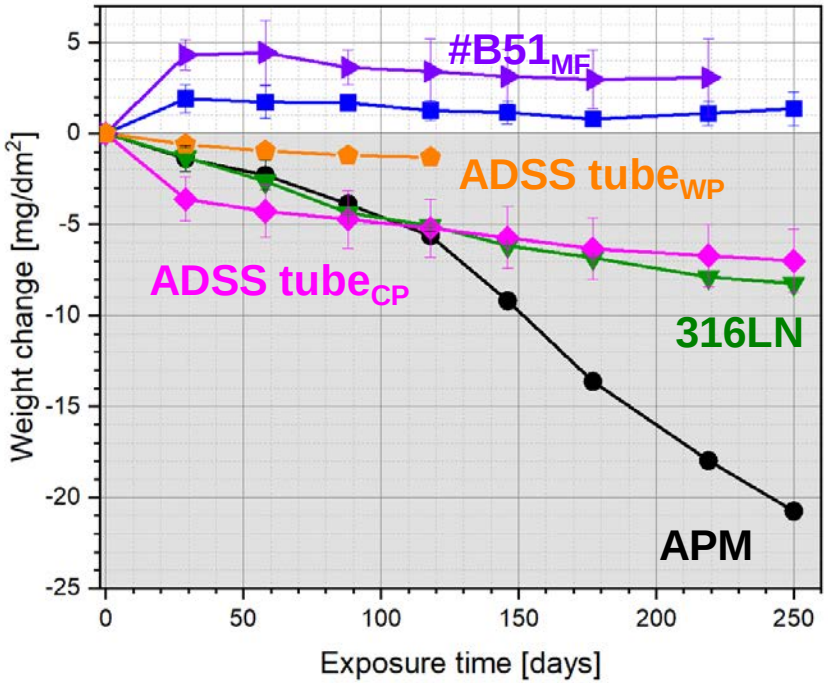

▲ Weight changes of Fe-base alloys in PWR environment at 360°C 190 bar for 8 months

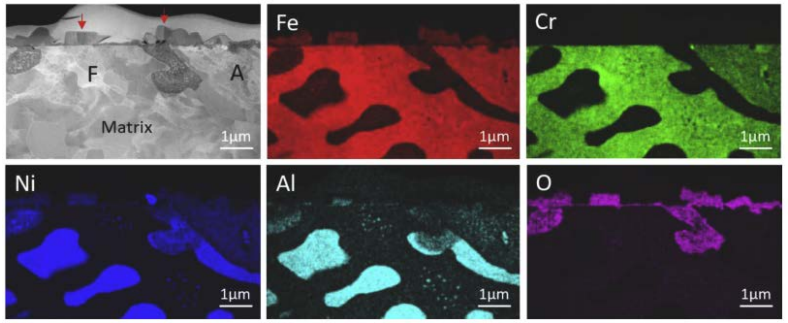

▲ STEM /EDS mapping results of oxide film formed on ADSS after PWR immersion test for 500 h [1]

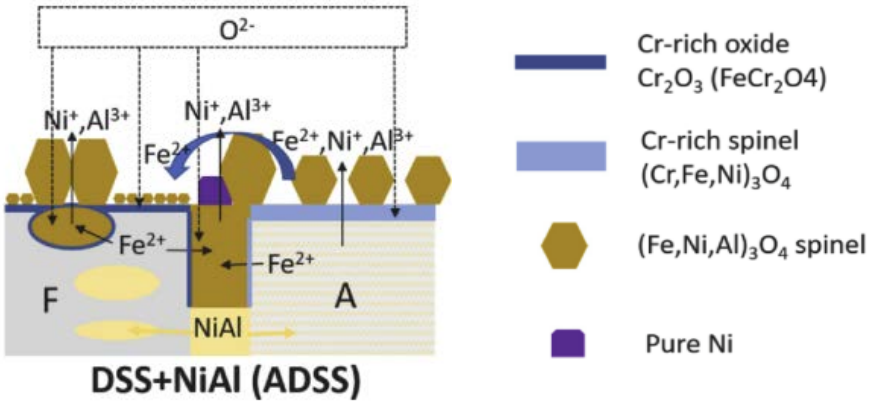

▲ Schematics of the oxide layer formation on ADSS in simulated PWR primary water [1]

Assessment related to normal operation

❑ Thermal ageing behavior at 400ºC for up to 6kh

- Depending on ADSS microstructure
- B2 in austenite and phase distribution → detrimental effect on thermal embrittlement

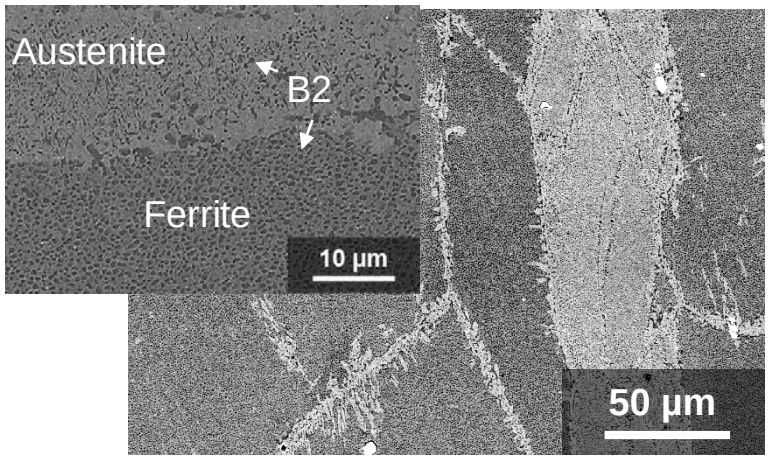

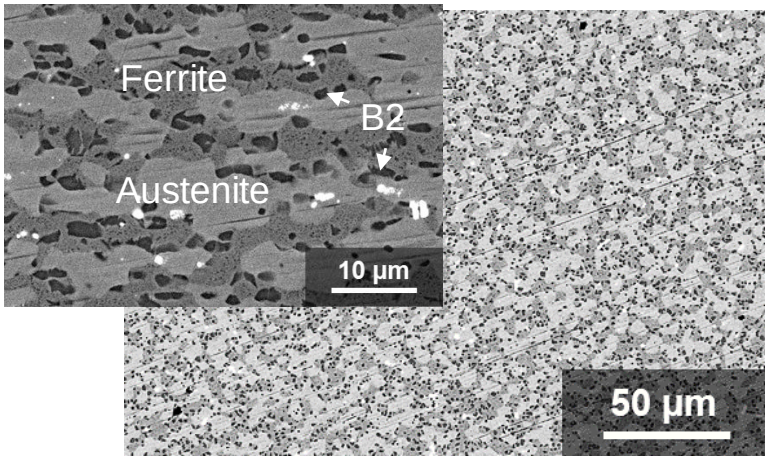

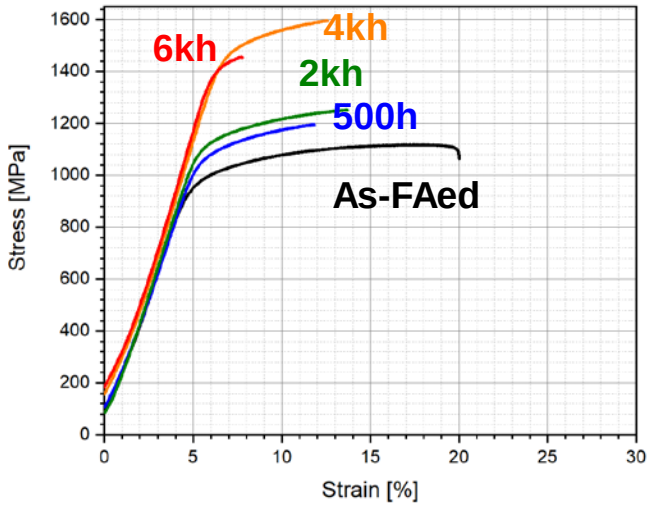

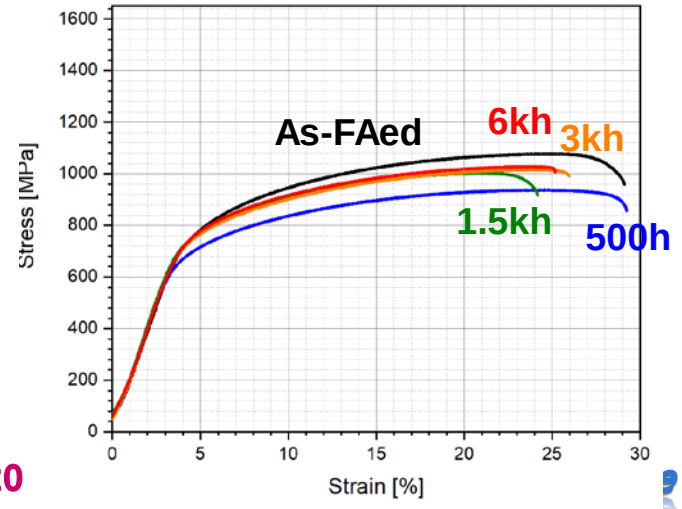

Assessment related to normal operation

❑ Phase stability in ferrite of ADSS at 375°C-475°C

- Austenite phase is stable & B2 in austenite is controllable
- Microhardness results: different ageing mechanisms in the temp. range
- 375°C & 400°C up to 6kh
  - Decomposition was not observed
- 425°C & 475°C
  - Cr-rich/Fe-rich BCC decomposition
  + ordered/disordered BCC decomposition

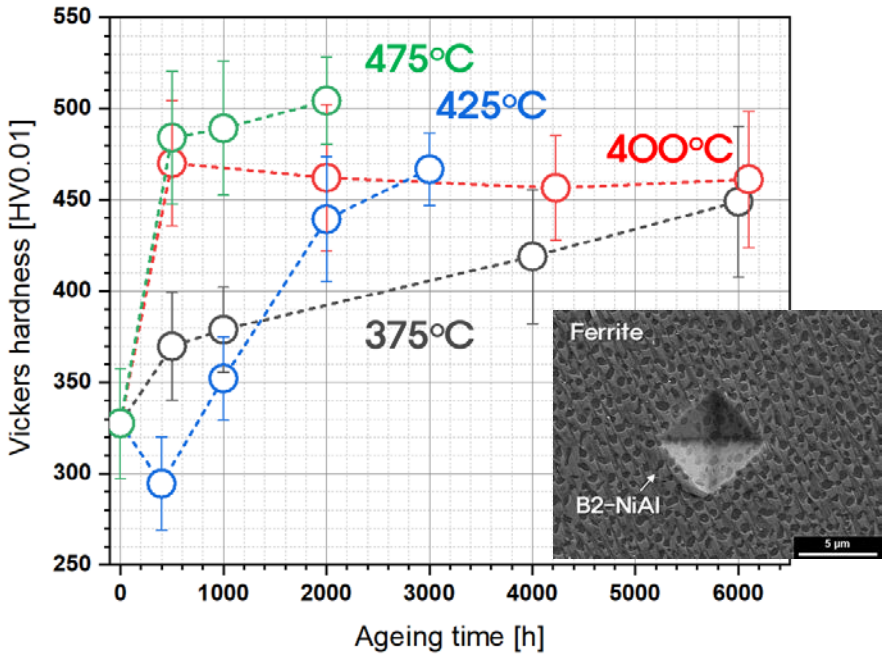

▲ Micro-hardness test results on ferrite of ADSS after thermal ageing

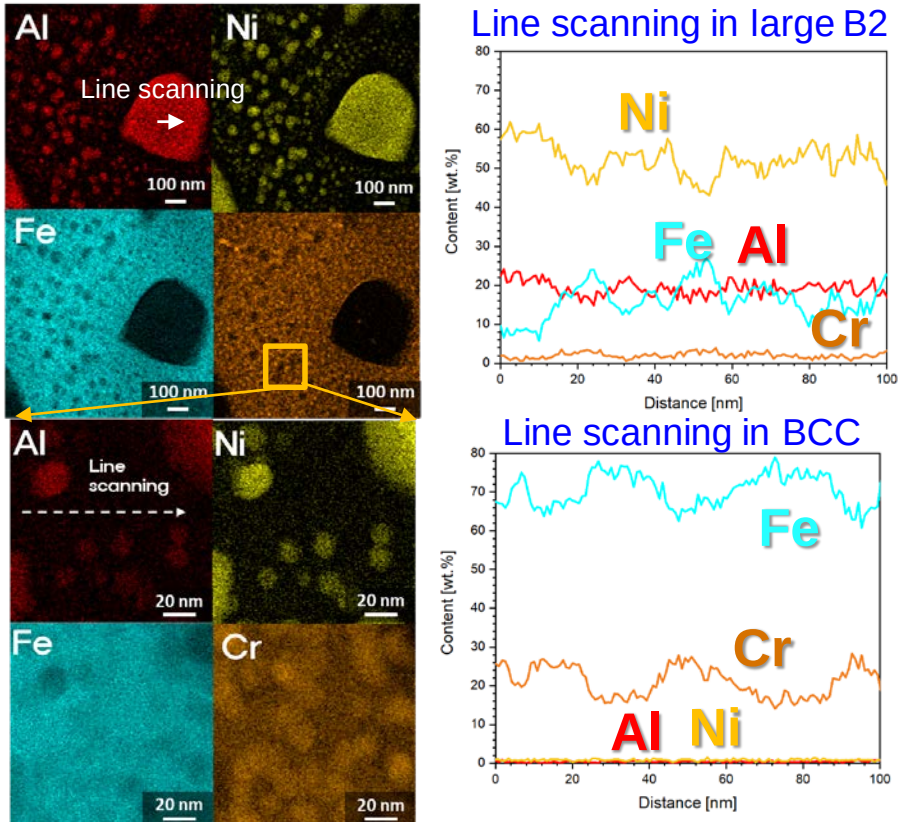

▲ STEM/EDS mapping and line scanning results of ferrite in ADSS after thermal ageing at 425°C for 3kh

Neutron penalty

[1] N.M. George et al., Ann. Nucl. Energy 75 (2015) 703-712
[2] C. Kim et al. Int. J. Energy Res. 44(10) (2020) 8074-8088

❑ Neutronic analysis of Fe-base ATF candidates

- High thermal neutron absorption c-x of transition elements (Ni, Cr, Fe)
- Westinghouse 17 × 17 PWR [1]
- PWR 16x16 PLUS7 fuel assembly using KARMA code in KEPCO NF for ADSS [2]
- Cladding thickness required for equivalent EOC value
  - 310SS ~226 μm with 4.90% of U-235 enrichment [1]
  - FeCrAl ~302 μm with 4.90% of U-235 enrichment [1]
  - ADSS >350 μm with 4.65 & 4.95% of U-235 enrichment [2]

▲ Fuel rod geometries for (left) current Zr-base alloys and (right) reduced cladding thickness and constant gap thickness

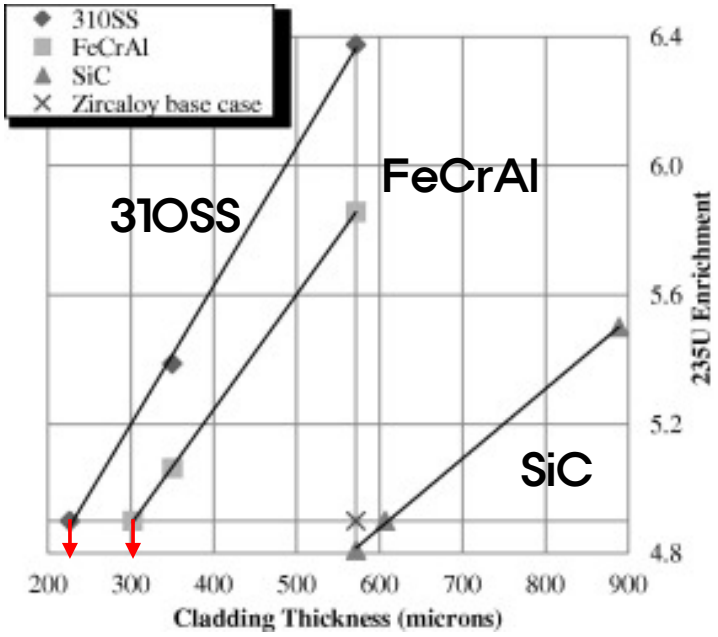

▲ Fuel parameters required to match the PWR life time [1]

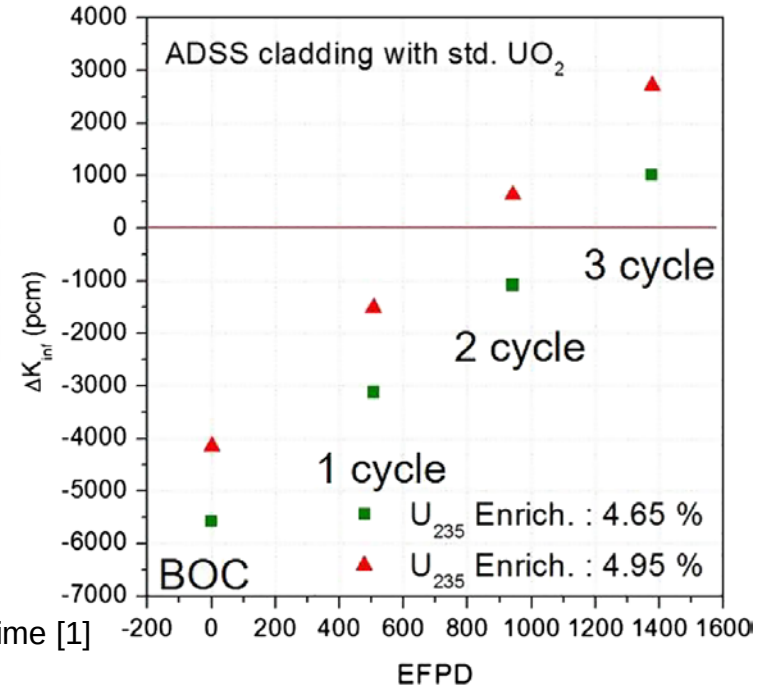

◀ Calculated reactivity and effect full power day (EFPD) for ADSS cladding with standard UO_2 cycles with different enrichments [2]

Further assessment of ADSS alloys in progress

Optimization of microstructure

❑ Preliminary stress corrosion cracking (SCC) behavior

- Steam SCC test at 400ºC in 20MPa using U-bend specimens
- One specimen of earlier heat was cracked among 3 specimens after steam exposure for 816h => Crack along loop-shape B2
- Microstrcture optimization in progress

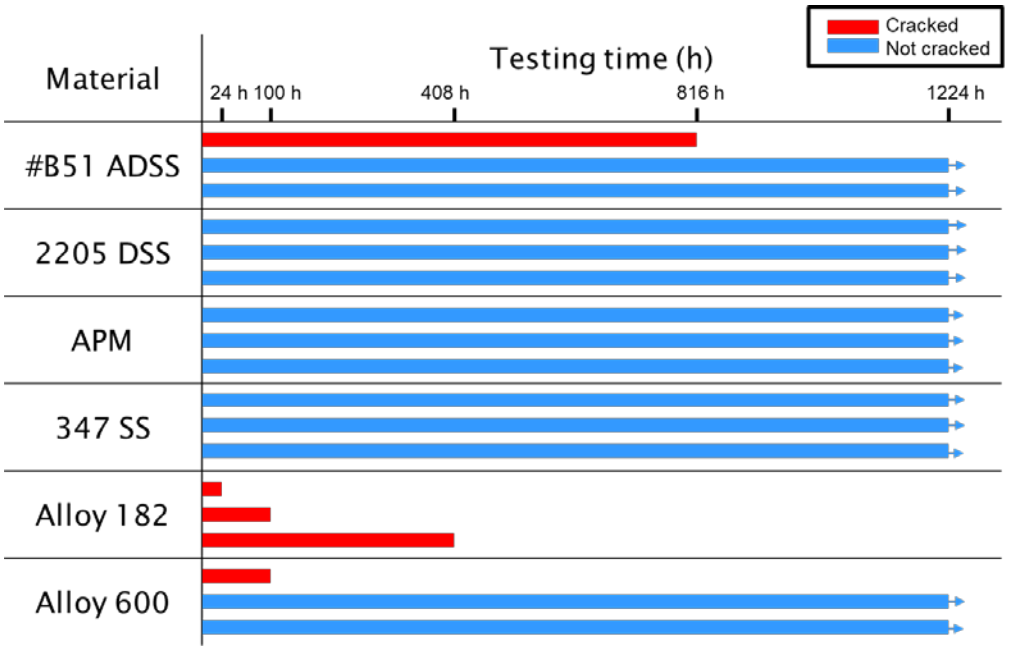

▲ Crack of U-bend specimens

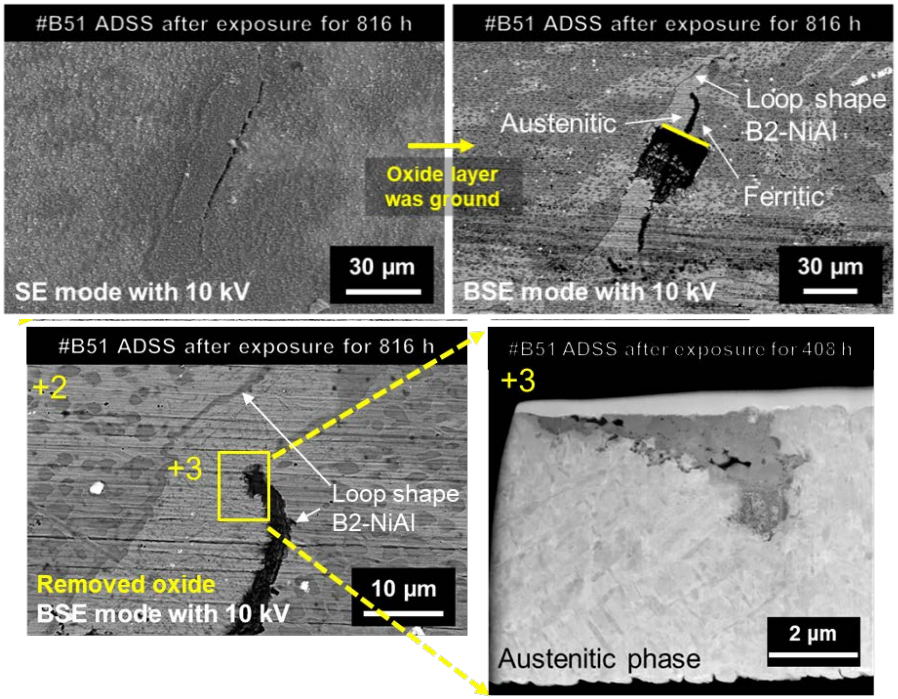

▲ Crack morphologies of ADSS #B51 after steam exposure at 400ºC for 816h

Optimization of microstructure

❑ Undesirable microstructures for ADSS alloys

- Loop-shape B2 for PWR corrosion and SCC
- Non-uniform phase distribution for thermal ageing
- Lots of B2 in austenite

❑ Optimized microstructure for ADSS alloys

- Uniform phase distribution and less B2 in austenite was achieved
  - By reducing Al content 6.1wt.% → 5.8 wt.%
- Now considering new thermo-mechanical process without reduced Al content for optimized microstructure

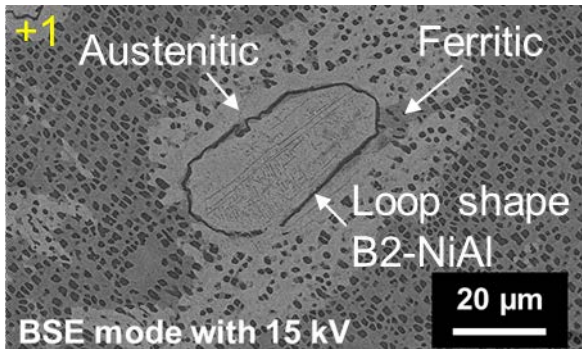

▲ Undesirable ADSS microstructure for PWR corrosion and SCC

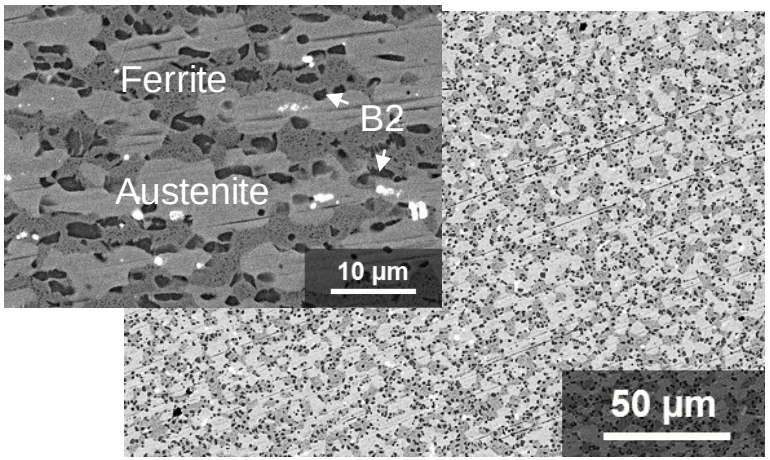

▲ Optimized microstructure of ADSS

Optimization of fabrication process

❑ Cold pilger process for thin ADSS tubes

- Multi-step with intermediate and final annealing
  - Currently, 10 steps for ADSS
  - 3 steps for Zr-claddings
- To simulate cold-pilger process, cold-rolling with intermediate annealing
- Intermediate annealing per 1 pass vs. 3 passes
  - 3 passes: more B2 in austenite & more-gathered phase distribution
- Plan to increase thickness reduction per 1 pass

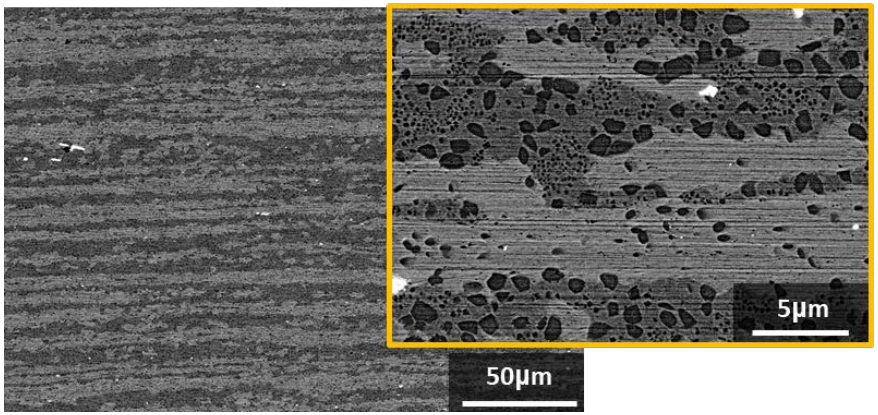

▲ Microstructures of ADSS cold-rolled with intermediate annealing per 1 pass (total 14 passes)

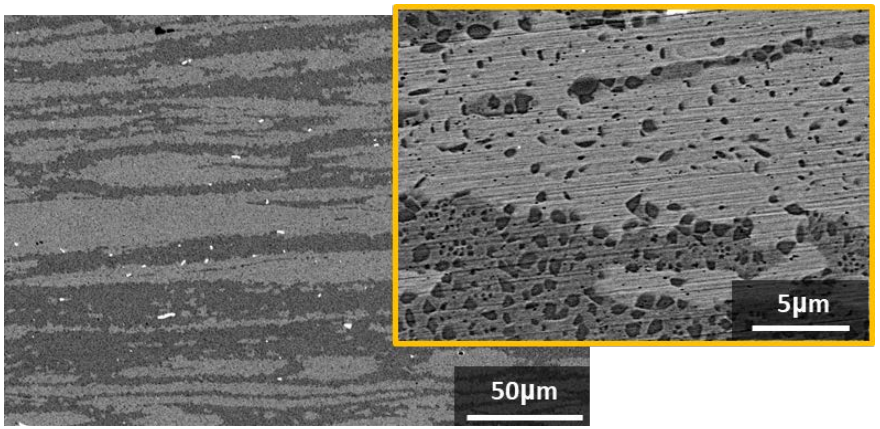

▲ Microstructures of ADSS cold-rolled with intermediate annealing per 3 passes (total 14 passes)

Summary

Summary

- **Development of alumina-forming duplex stainless steels (ADSS)**
  - Nominal composition of Fe-(16-20)Ni-16Cr-(5.5-7.0)Al + minor elements
    - Austenite(FCC), ferrite(BCC), nickel aluminide (B2-NiAl) co-exist
  - Protective oxide layers in both normal and accident conditions
  - High strength (UTS ~ 1GPa) and reasonable ductility (UE ~ 15 %)
  - 0.3mm-thick 4m-long cladding was successfully fabricated by cold-pilger

- **Further assessment of ADSS**
  - Steam oxidation at 800-1050^{o}C
    - Similar weight gain with APM
  - High temperature mechanical properties
    - UTS ~ 800MPa at up to 500^{o}C
    - Much smaller creep rate than Zr at 650^{o}C and 1000^{o}C
    - No burst and ballooning up to 1200^{o}C (hold 480s at 1200^{o}C)
  - PWR corrosion behavior
    - Saturated weight changes after 30days-exposure
    - $(Fe,Ni,Al)_3O_4$ formed along large B2

Summary

❑ Issues of ADSS

- Thermal ageing behavior at 375 ~ 400°C
  - Less significant and quickly saturated
  - Fine-distributed phase and B2-free austenite → mitigate thermal ageing embrittlement
- SCC behavior
  - One among three specimens of earlier heat was cracked after PWR steam immersion for 816h => Crack along loop-shape B2 => Microstructure optimization in progress
- Thermal properties
  - Melting point ~1420°C
  - Phase transformation at ~530°C and ~1000°C

❑ On-going optimization researches of ADSS

- Fine-distributed phase and B2-free austenite
  - By reducing Al, optimized microstructure is obtained
  - Try to obtain the microstructure without Al decrease
- Less steps cold-pilger process
  - Currently, 10 steps for ADSS tube
  - Reduction of passes by increasing thickness reduction per 1 pass
- IASCC resistance
  - Proton irradiation ~ 5 dpa in progress at MIBL

Summary

Good	Bad	Remark
High strength	Neutron penalty	~ 20% in fuel cost
Ductility	Low melting T	
Creep & rupture	Thermal ageing	Microstructure & Property optimization
No H embrittlement	High strength	
	T permeation	Oxide layer may help

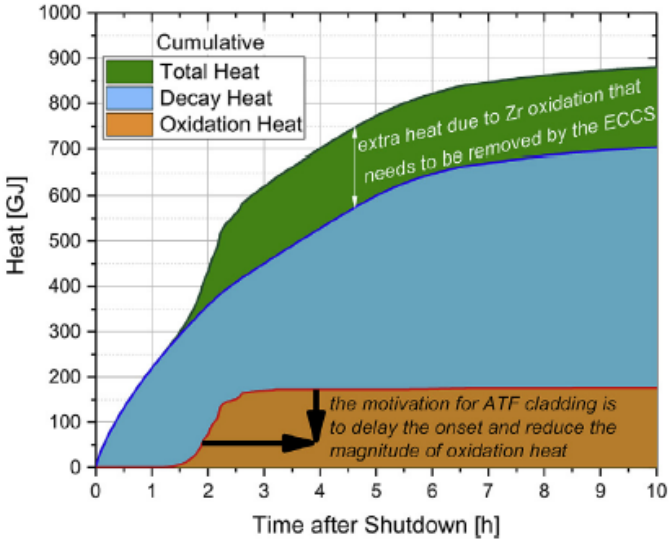

"ADSS"		Cladding				
		NO	PR	LOCA	RIA	SBO
Thermal conductivity	High	↑	↑	↑	-	-
Heat capacity	High	-	-	↑	-	↑
Oxidation rate	Low	↓	↓	↓	↓	↓
Coefficient of thermal expansion		-	-	-	-	-
Creep rate	Low	↑	↑	↓	-	↓
Strength	High	↑	↑	↑	↑	↑
Critical heat flux (CHF)	High	↑	↑	-	↑	-

KAIST

NQe Department of Nuclear & Quantum Engineering

NU_Html Nuclear & High Temperature Materials Laboratory

Energy for Earth !!

Thank you!

(Extra) Performance in molten salts

- **Preliminary KCl-$MgCl_2$ corrosion test at 700°C for 100h**
  - **Collaboration with Prof. S.Y Choi (SNU)**

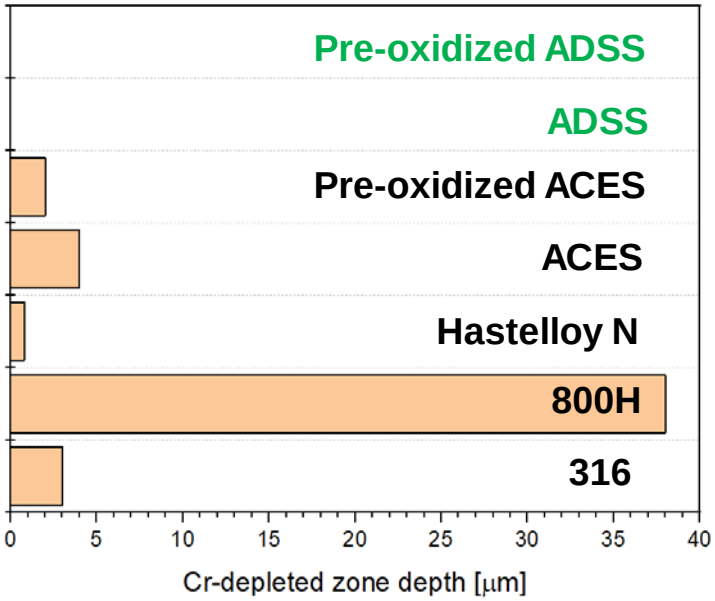

▲ Cr-depleted zone of alloys used in the test

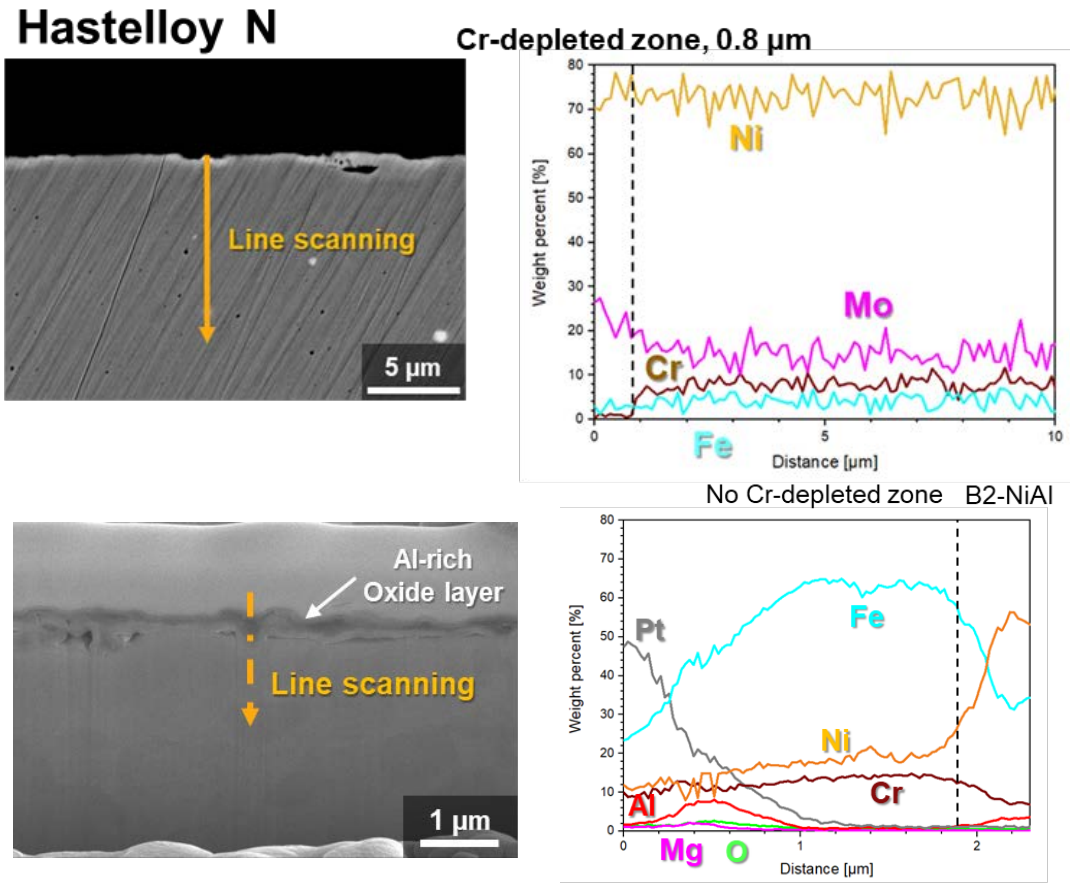

▲ Cross-sectional SEM images and EDS line scanning results for (top) Hastelloy N and (bottom) ADSS

(Extra) Performance in molten salts

❑ Long-term test plan for molten salt corrosion

- Materials (6)
  - 316H, Hastelloy N
  - ACES, Pre-oxidized ACES / ADSS, Pre-oxidized ADSS
- Change molten salt
  - $KCl\text{-}MgCl_2$ → KCl-NaCl
- Change test temperature and time
  - 700°C for 100h → **750°C for 500h**
- Change test zone
  - Individual salt for each sample → large cylindrical test zone for all samples

▲ Individual salt for each sample in a glove box

▲ large cylindrical test zone for all samples a glove box

App. Tensile properties of ADSS alloys

H. Kim et al. J. Nucl. Mater., 507 (2018) 1

❑ Mechanical properties

- Cold-rolled (CR) + final annealed (FA) (900°C 30min FC)

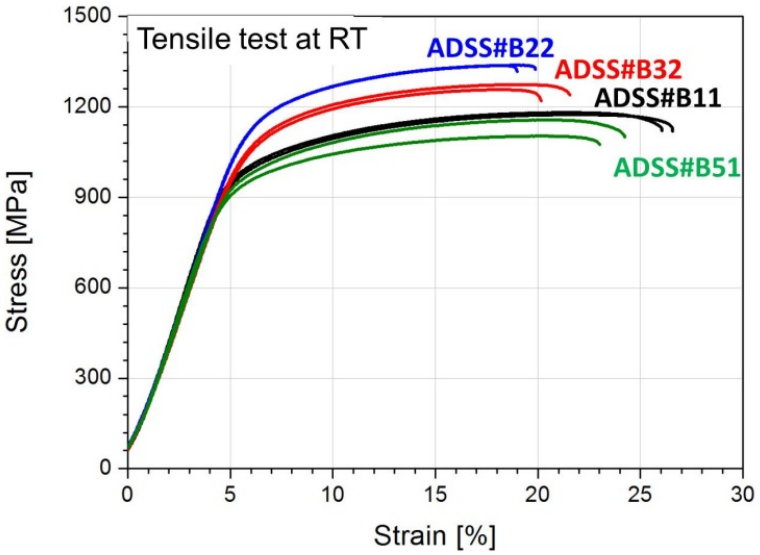

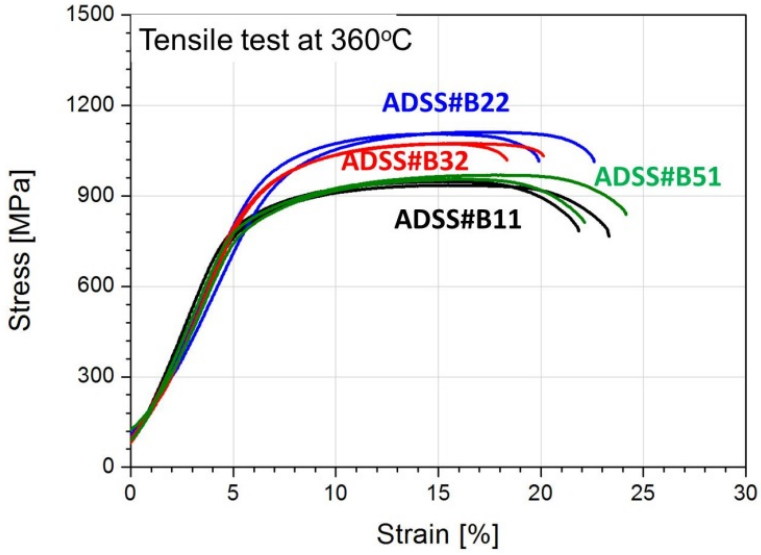

Materials (grade)	Yield strength [MPa]	Tensile strength [MPa]	Elongation [%]
Zircaloy-4	298 ± 9	481 ± 1	18.2 ± 0.6
APM (FeCrAl)	528 ± 19	698 ± 13	11.9 ± 0.6
310S	299 ± 8	580 ± 15	51.9 ± 1.1
DSS2205	629 ± 24	830 ± 24	34.2 ± 1.2
ADSS B11	929 ± 30	1198 ± 10	20.5 ± 0.4
ADSS B51	**929 ± 30**	**1129 ± 38**	**18.5 ± 0.8**

App. Assessment related to accidents

[1] J. Nucl. Mater. 491 (2017) 55-66

❑ Thermal properties

- DSC analysis
  - Measured up to 1000°C with heating rate of 10°C/min to determine phase transition temperature
    - Phase transformation at ~ 530°C
    - Would be related to the loss of strength
  - Measured up to 1470°C with heating rate of 30°C/min to determine melting point
    - Melting point 1416- 1424°C (FeCrAl ~ 1525-1540°C [1])

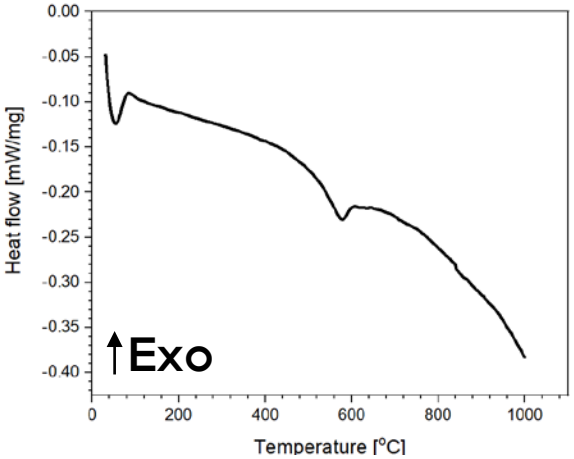

▲ DSC analysis result of ADSS up to 1000°C during heating with a rate of 10°C/min

- Thermal conductivity, k
  - k = thermal diffusivity * heat capacity * density
  - Density of ADSS = 7.248 g/cm^3 at RT
  - Reduced k at 1000°C due to phase transformation

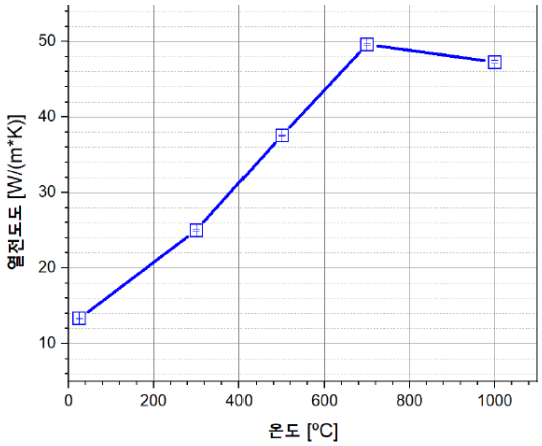

▲ Thermal conductivity of ADSS up to 1000°C